



Alternating Magnetic Field Effect on Fine-aggregate Concrete Compressive Strength



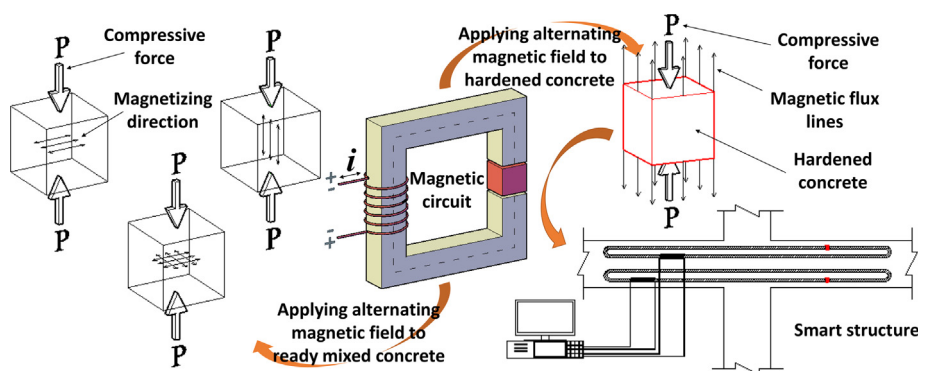
Iman Abavisani, Omid Rezaifar*, Ali Kheyroddin

Department of Civil Engineering, Semnan University, Semnan, Iran

HIGHLIGHTS

- Devising a specialized test setup comprising gapped magnetic circuit.
- Increase in compressive strength by 7.78% due to exposing hardened concrete to AMF.
- A marginal effect of exposing fresh concrete to AMF on the compressive strength.
- The ability of this method as a base for a new generation of smart structures.

GRAPHICAL ABSTRACT



ARTICLE INFO

Article history:

Received 20 May 2016

Received in revised form 30 October 2016

Accepted 21 December 2016

Keywords:

Alternating Magnetic Field (AMF)

Concrete

Compressive strength

Magnetic circuit

Magnetic flux density

ABSTRACT

An exploratory investigation was conducted into the feasibility of using Alternating Magnetic Field (AMF) to enhance concrete compressive strength and to invent a new actuators system in smart structures. Hence, some small-scale experiments were performed on cube fine aggregate concrete specimens, wherein the effect of applying AMF of density 0.5 Tesla (T) and frequency 50 Hz to ready mixed and hardened concrete on the compressive strength was examined. Besides, the role of the direction of AMF applied to ready mixed concrete in changing its physical behavior was evaluated. For exposing the specimens to AMF, a specialized magnetic circuit was designed. It was observed that applying AMF to fresh concrete has a marginal effect on compressive strength. But, exposing hardened concrete enhanced the compressive strength up to 7.78%. The advantage of this effect was discussed theoretically from different aspects. It was found that this method can be a base for behavior controlling of large-scale smart concrete structures in real time, through adjusting element stiffness by AMF. Finally, the feasibility of this method for large-scale RC structures was explained, giving a graphical example.

© 2016 Elsevier Ltd. All rights reserved.

1. Introduction

Enhancing stability of concrete structures is a vital issue in structural engineering having led to invention of different ways

such as making structures smart against dynamic forces and improving physical properties of concrete. To attain these goals various methods such as using chemical admixtures and fine aggregate materials known as nano-particles have been widely investigated (for example [1]). Recently, profiting from electromagnetism has been widely used to improve concrete properties.

As to smart structures, electromagnetism has been used mostly in structure performance monitoring [2,3]. Smart structures

* Corresponding author.

E-mail addresses: iman.abavi@yahoo.com (I. Abavisani), orezayfar@semnan.ac.ir (O. Rezaifar), kheyroddin@semnan.ac.ir (A. Kheyroddin).

include some sensors and actuators systems comprising smart materials such as Fiber Optics (FOs) [4–6], piezoelectrics [7–9], Magneto-Rheological (MR) materials [10,11], Electro-Rheological (ER) materials [12,13], Shape Memory Alloys (SMAs) [14,15]. The performance of such structures depends on the utilized smart material properties. This technology has been used for applications such as damage detection, shape control [16,17], noise and acoustic control [18,19], health monitoring [20,21], vibration control [22,23], and energy harvesting [24,25]. These techniques, however, have their own shortcomings for example unsuccessfulness at early stages of damage, difficulty in sensor installation, reduction in load-bearing capacity of the element due to taking up too much space in it, distinction between the load bearing system and the sensors [26].

Regarding concrete properties improvement, a novel method is magnetic treatment of concrete water. This method is based on the effect of magnetic field on water properties explained by Lorenz in 1902 for the first time. When water is exposed to magnetic field, the consolidation degree between water molecules decreases and the size of the molecules increases [27], thereby changing some of its physical and chemical characteristics such as viscosity, solubility, temperature, specific weight, surface tension, electric conductivity, PH, permeability pressure [28,29]. Most of studies in this field have concluded that using magnetized water in concrete fabrication increases the compressive strength by 10–25 percent and also improves concrete workability [30–36]. This causes that in some cases, with the same compressive strength and workability, the cement content can be reduced. According to one of recent studies, this reduction can fall to 28% [30]. In addition, using magnetic water in concrete makes it more resistant to freezing and permeating and increases its plasticity [31]. Magnitude of such changes is controlled by some factors such as treatment duration and the power of magnetic field. It is shown that if water is subjected to a magnetic field of intensity 0.985 T for 24 h, the compressive strength can increase up to 55% besides a slight increase in workability [37].

Recently, the effect of applying magnetic field to ready mixed concrete comprising carbonyl iron powder (as MR material [38]) on its fresh-state properties was studied. It was found that this method changes the shear resistance of concrete but has no effect on the compressive strength [39]. According to another recent investigation dealing with the effect of static magnetic field of different powers up to 25.37 Gauss, ($1 \text{ Gauss} = 10^{-4} \text{ T}$), on cement paste properties, at different ages up to 7 days of hardened cement pastes samples, it was found that the amount of Calcium Silicate Hydrate (CSH) gel is larger and its morphology becomes denser and less porous with higher magnetostatic induction strength; magnetic field changes the mineralogical composition of hydrated cement pastes and enhances mechanical strength of cement pastes where the maximum increase in compressive strength equal to 13% was observed as to the 7-day aged specimens having been treated by magnetic field of strength 25.37 Gauss [40].

However, studies on the effect of directly applying magnetic field to cementitious materials on their physical properties are very scarce in technical literature. Moreover, the use of magnetic fields for concrete containing smart materials is almost limited to the effect of static magnetic field applied to fresh cementitious materials on their fresh state properties. Up to the authors knowledge, there have been no studies dealing with (a) the effect of Alternating Magnetic Field (AMF) applied to ready mixed concrete, (b) the effect of the direction of AMF applied to ready mixed concrete, (c) the effect of applying AMF to hardened concrete, on its physical properties.

This study aims to uncover these facts and explore feasibility of making a new generation of smart concrete structures using AMF, performing some small-scale experiments on different fine aggregate

concrete specimens. The procedure is divided into two phases: I) the fresh-state phase including the effect of exposing fresh concrete to AMF on the compressive strength; the role of the direction of AMF applied to fresh concrete in hardened concrete behavior, II) the hardened-state phase including the effect of applying AMF to hardened concrete on the compressive strength.

2. Research significance

Different ways for promoting physical properties of concrete have been widely dealt with. However, the authors believe that the effect of directly applying magnetic field to concrete on its mechanical properties as well as the use of magnetic fields in controlling concrete structural behaviors in real time have not been addressed. Hence, the present study is to deal with these issues for the first time. The consequence of this exploratory investigation can be used in real time behavior controlling of smart structures, with financial and practical advantages over some existing methods like no need for actuators systems installation in concrete.

3. Experimental investigation

3.1. Materials

Throughout the investigation the AMF used was of frequency 50 Hz with a magnitude of 0.5 T. The cement used in all the specimens was commercial ordinary portland cement the chemical and physical properties of which are given in Table 1. The aggregates used were air dried river sand of maximum particle size 2.36 mm [0.093 in.]. To improve workability of specimens, all the samples were prepared using superplasticizer with the same dosages. The water mixed was tap water. To avoid from a high amount of magnetic leakage because of the high magnetic permeability of steel materials; and for almost all of magnetic flux to pass through molded fresh concrete, for all specimens plastic molds of thickness 3 mm [0.12 in.] were used.

3.2. Test program

Fifteen fine aggregate concrete specimens were examined for compressive strength. The main variables in the test series include: a) AMF exposure occasion, and b) AMF exposure direction. As to variable (a), the specimens were divided into three types including: Non-Magnetized (NM) specimens which were not exposed to AMF, Pre-Magnetized (PrM) specimens which AMF was applied to fresh concrete immediately after casting concrete into molds, Post-Magnetized (PoM) specimens in which the specimen was exposed to AMF after hardening, during the test. Variable (b) is associated with the PrM specimens, depending on magnetizing direction as explained in Table 2 and shown in Fig. 1.

Table 1
Physical and chemical properties of cement.

Compressive strength, 28 days, MPa	45
Specific surface, Blaine, m^2/kg	300
SiO_2 , %	20.6
Al_2O_3 , %	5.6
CaO, %	63.0
MgO, %	2.7
SO_3 , %	2.3
Na_2O , %	0.6
K_2O , %	0.7
LOI, %	1.7
Fe_2O_3 , %	3.95

Note: 1 MPa = 145 psi; $1 \text{ m}^2/\text{kg} = 0.542 \text{ yd}^2/\text{lb}$.

Table 2
AMF exposure directions for PrM specimens.

Exposure direction	Explanation
(→ - ←)	Compressive force and AMF were applied to the specimen in the same directions (Fig. 1(a))
(→ ←)	Compressive force was applied to the specimen perpendicular to the direction of AMF (Fig. 1(b))
(→ + ←)	AMF was applied to the specimen in two perpendicular directions and compressive force was applied perpendicular to the magnetization plane (Fig. 1(c))

All specimens of the study are listed in Table 3. In the table, specimens are labeled based on the aforementioned variables. The first and second parts of the labels are associated with the variables (a) and (b), respectively. For example, the specimen labeled PrM (→ | ←) stands for a Pre-Magnetized specimen that AMF is applied to ready mixed concrete as (→ | ←).

3.3. The magnetic circuit employed: explanations and calculations

The used AMF generator machine consists of a solenoid made up of a wire wound into a coil with a core of iron as a ferromagnetic material, as shown in Fig. 2.

Consider the simple magnetic circuit shown in Fig. 3(a). The magnitude of the magnetic field known as magnetic flux density is defined as:

$$B = \frac{\varphi}{A} \tag{1}$$

where B , φ , and A are the magnetic flux density in (T), the magnetic flux in Weber (Wb), and the cross-sectional area of the circuit in (m^2), respectively. The Magneto Motive Force (MMF) which drives magnetic flux through the circuit is defined as:

$$F = NI \tag{2}$$

where F , N , and I are MMF measured in ampere-turn (At), the number of turns of the coil, and the electric current through the coil in amperes (A), respectively. The magnetic reluctance of the circuit is obtained as follows:

$$R = \frac{F}{\varphi} \tag{3}$$

where R is the magnetic reluctance of the circuit measured in inverse henry (H^{-1}). The reluctance of a magnetic element can be calculated as:

$$R = \frac{l}{\mu A} \tag{4}$$

where

l is the length of the element measured in (m).

$\mu = \mu_r \mu_0$ is the magnetic permeability of the material measured in henries per meter ($H.m^{-1}$),

μ_r is the relative permeability of the material which is dimensionless, and μ_0 is the permeability of free space which has the value of $4\pi \times 10^{-7} H.m^{-1}$.

A is the cross-sectional area of the element in (m^2).

The Eqs. (3) and (4) are used for Direct Current (DC) fields. In the case of Alternating Current (AC) fields, the magnetic complex reluctance is the case of interest. So these equations are replaced by Eqs. (5) and (6), respectively [41,42].

$$Z_\mu = \frac{\dot{N}}{\dot{\varphi}} = \frac{\dot{N}_m}{\dot{\varphi}_m} \tag{5}$$

$$Z_\mu = \frac{l}{\dot{\mu} \mu_0 S} \tag{6}$$

where

Z_μ is the magnetic complex reluctance.

\dot{N} and \dot{N}_m represent the amplitude of the MMF.

$\dot{\varphi}$ and $\dot{\varphi}_m$ represent the amplitude of magnetic flux in the circuit.

$\dot{\mu} \mu_0$ is the complex magnetic permeability.

S is the cross-section of the element.

Regardless of what kind of magnetic flux flowing through the circuit, reluctance is directly proportional to the length of the circuit while inversely proportional to its cross-sectional area and permeability [43].

For magnetizing of the concrete specimens, a magnetic circuit with a gap was designed as shown in Fig. 3(b). The concrete specimen was aimed to be put in the gap while magnetizing. In this condition the cores of iron and concrete form a single circuit with

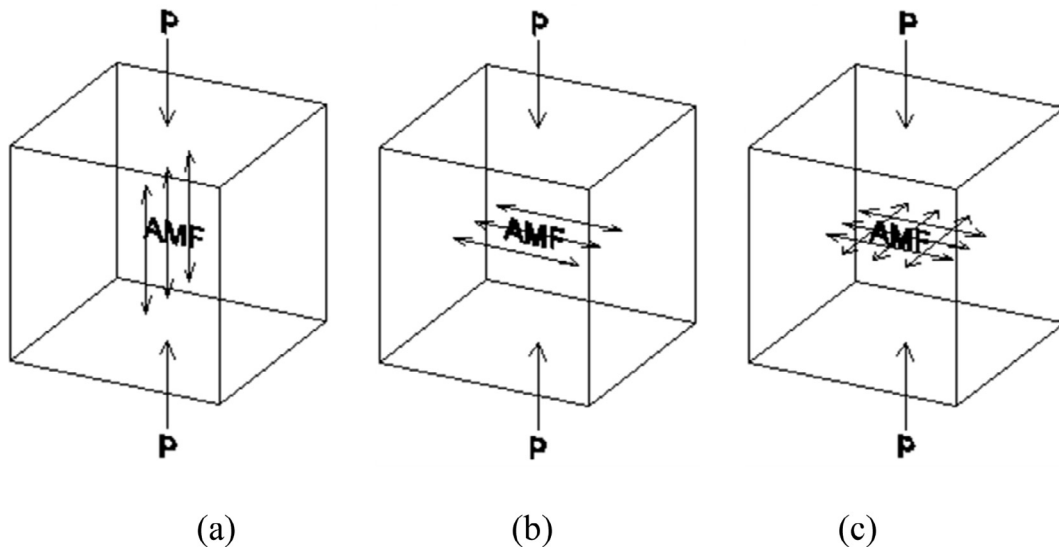


Fig. 1. The direction of AMF applied to PrM specimens.

Table 3
Total list of experimental specimens.

Specimen type	AMF (Tesla)	Number of specimens
NM	0	3
PrM ($\rightarrow - \leftarrow$)	0.5	3
PrM ($\rightarrow \leftarrow$)	0.5	3
PrM ($\rightarrow + \leftarrow$)	0.5	3
PoM	0.5	3

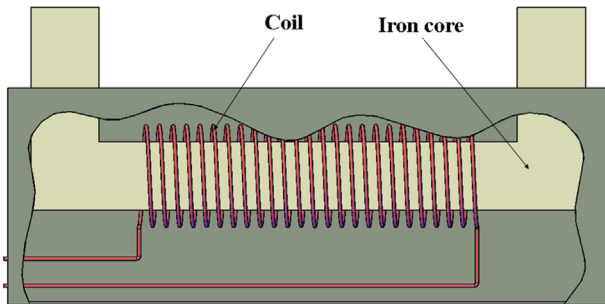


Fig. 2. The AMF generator machine.

two components connected in series. In this circuit the amount of φ remains the same throughout the circuit and is calculated as:

$$\varphi = \frac{F}{R_T} \quad (7)$$

where R_T is the total reluctance of the circuit, calculated as [43]:

$$R_T = R_i + R_c \quad (8)$$

where R_i and R_c are the reluctances of iron and concrete elements, respectively. In this study the number of wire turns and current intensity are constant, thus F remains constant. So, according to Eq. (7) the only possible way to prevent flux reduction is to keep the total reluctance at the lowest possible amount. As an approximation, magnetic permeability of concrete zone can be assumed equal to that of free space μ_0 . The permeability of iron μ_i is very high compared to μ_0 . This causes R_c become very large compared to R_i , resulting in a considerable reduction of magnetic flux. According to Eq. (4) and/or Eq. (6), the practical way to offset, to some extent, this adverse effect regarding μ_0 is to keep the length of the concrete zone as small as possible. Hence, in order to enhance the reliability of the results in the present study small concrete specimens of size $50 \times 50 \times 50$ mm [$2 \times 2 \times 2$ in.] were planned to be exposed to AMF.

3.4. Specimens

All specimens were prepared according to the mix proportions given in Table 4. For preparing the specimens, the Supelastizer was firstly dissolved in water. Then, cement and aggregates were hand mixed at a low speed for 2 min. After that, the ready mixture of water and superplasticizer was poured in and stirred at a low speed for several min. And finally, the well-mixed concrete mixture was poured into the molds. Immediately after that, the PrM specimens were magnetized according to the predetermined magnetizing directions for 2 min as shown in Fig. 4. As can be seen, to prevent the terminals of the AMF generator from touching and shaking the molds during magnetization there were small distances between the molds and the two terminals. All specimens were compacted with a steel bar of diameter 3 mm [0.12 in.].

For the PrM ($\rightarrow + \leftarrow$) specimens to be magnetized, the molds were, continually every about two seconds, taken off the position and turned by 90° and then were put in position. The specimens were de-molded after 24 h and cured in water at about 20°C [68°F].

3.5. Test procedure

After 28 days, the specimens were examined for compressive strength as per ASTM C109 [44]. To make sure that AMF did not affect the sensors of the testing machine during testing of PoM specimens, a non-digital measuring machine was used for all specimens.

As to assembling the test setup for PoM specimens, they were put between two cylindrical steel pieces of diameter 70 mm [2.7 in.], hence concentrating almost all of AMF through the specimens, and minimizing magnetic leakage. In order for experimental condition to remain identical, all specimens were put between

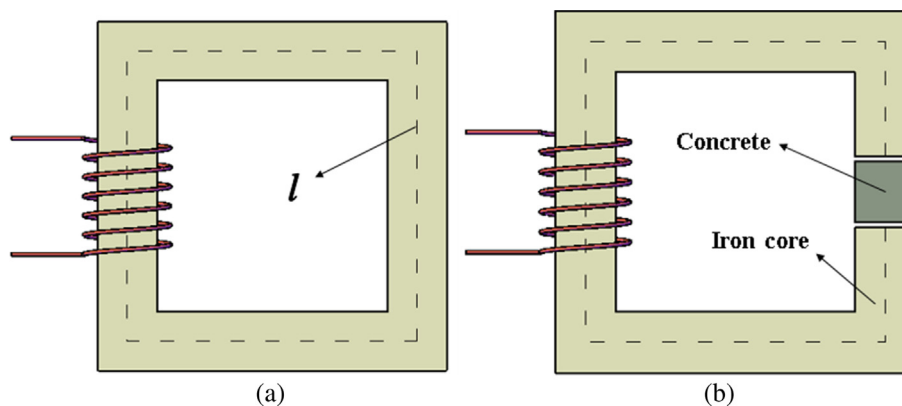


Fig. 3. a) a simple magnetic circuit, b) The gapped magnetic circuit of the study.

Table 4
Mix proportions of the samples.

Water (kg/m ³)	Cement (kg/m ³)	W/C	Sand (kg/m ³)	Superplasticizer (lit/m ³)
292.5	450	0.65	1700	20

Note: 0.4536 kg = 1 lb, 0.0254 m = 1 in., 1 lit = 61.026 in.³.

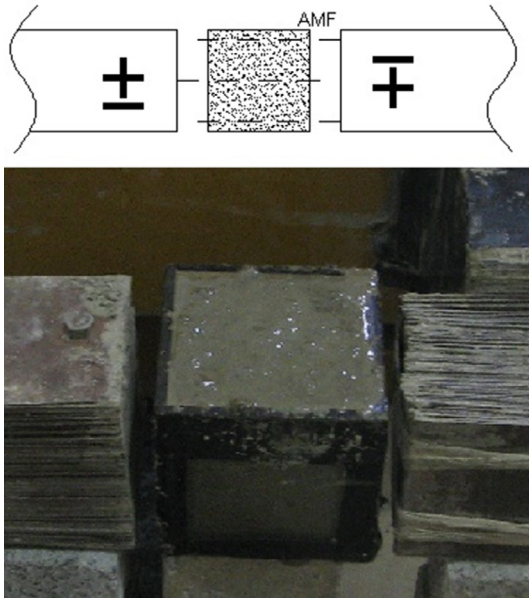


Fig. 4. Magnetizing of PrM specimens.

these plates while testing. The test setup for PoM specimens is shown in Fig. 5. For applying AMF, the terminals of AMF generator were put in touch with the upper and lower platens of the measuring machine. For testing each PoM specimen, AMF was applied during the test until the specimen collapsed.

4. Results and discussion

4.1. Experimental results and discussion

While PrM specimens were exposed to AMF, small vibratory movements were observed in fresh fine aggregate concrete in the

molds. These movements may have arisen from the existence of charged particles in the aggregates and/or cement.

The averaged results of compressive strength of specimens are given in Table 5. Enhanced extent in the compressive strength for all of them is illustrated in Fig. 6. Considering the results of NM and PrM specimens it can be seen that the maximum difference in strength between them is around 1%. Thus, it seems that magnetizing of ready mixed concrete has had a negligible effect on concrete behavior.

The results of PoM specimens show that applying AMF to hardened concrete has increased its compressive strength by 7.8%. It seems that AMF has affected microstructure of hardened concrete, making microscopic charged particles in concrete matrix orient in the direction of AMF, enhancing its compressive strength. This observation implies that magnetizing fresh concrete may have affected its microstructure during exposure too, but thereafter in the absence of AMF it may have got back into the former state. This may be the reason why compressive strength of PrM specimens was close to that of NM ones.

The effect of AMF on hardened concrete properties can be useful in different aspects and utilized to control behavior of structures in real time through employing magnetic fields when dynamic forces occur.

4.2. Compression test results of PoM specimens: theoretical discussion

The results of PoM specimens can be discussed as to large-scale concrete structures from different aspects of concrete building code. Below, the effect of applying AMF to hardened concrete, when strong forces occur, on some items such as minimum reinforcement ratio, elastic modulus, relation between stress and strain, ductility, and nominal moment strength of concrete as per ACI318-2014 [45] is dealt with. Note that all ACI formulae are based on compressive strength of cylindrical concrete specimens, but nevertheless using the strength results of cube specimens of the present study for the following discussions makes no anomaly or deviation for the overall results.

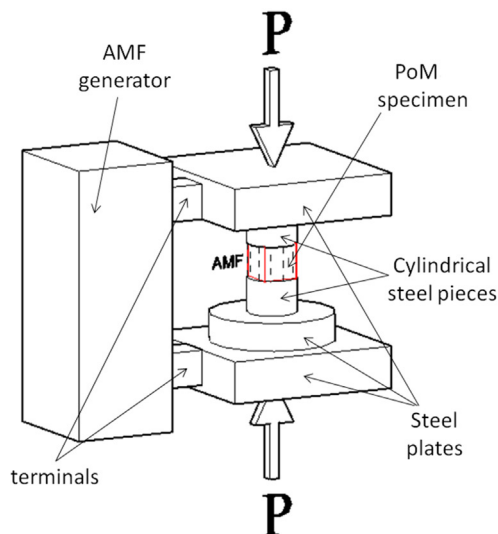


Fig. 5. The test setup for a PoM specimen.

Table 5
Compressive test results of specimens.

Specimen label	Compressive strength (MPa)	Standard deviation (σ)	Enhanced extent (%)
NM	20.6	0.18	0
PrM ($\rightarrow - \leftarrow$)	20.5	0.15	-0.48
PrM ($\rightarrow \leftarrow$)	20.8	0.12	0.98
PrM ($\rightarrow + \leftarrow$)	20.8	0.06	0.98
PoM	22.2	0.26	7.77

Note: 1 MPa = 0.145 ksi.

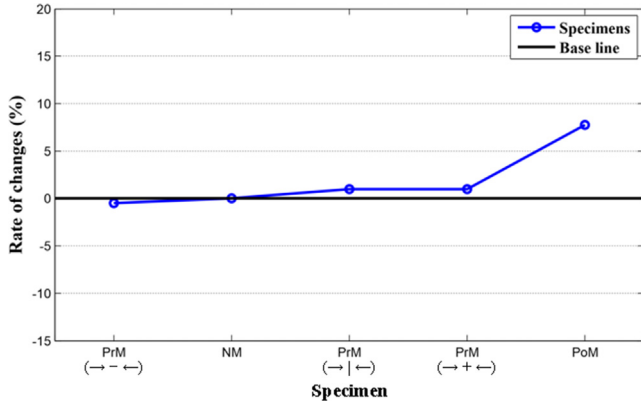


Fig. 6. Enhanced extent in compressive strength of the specimens. (Note: 1 MPa = 0.145 ksi).

- Minimum reinforcement ratio

The minimum reinforcement ratio for designing of Reinforced Concrete (RC) beams is calculated as [45]:

$$\rho_{\min} = \frac{\sqrt{f'_c}}{4f_y} \geq \frac{1.4}{f_y} \quad (9)$$

where f'_c and f_y are, respectively, the concrete compressive strength and the reinforcement yield strength in MPa. If $f'_c \geq 31$ MPa ($f'_c \geq 4.495$ ksi), the term of $\frac{\sqrt{f'_c}}{4f_y}$ is determinative. From the PoM results, it can be said that by magnetizing RC beams made of concrete with $f'_c \geq 31$ MPa ($f'_c \geq 4.495$ ksi), when strong dynamic forces occur, the cube strength (f'_{cu}), and as a result, f'_c increases by 7.77%. Therefore, according to Eq. (9) ρ_{\min} can be considered about 3.8% less than usual.

- Concrete stress-strain relation

A lot of models have been proposed by several researchers to show stress-strain relation of concrete, among which the one proposed by Hognestad [46] is one of the most commonly used models as shown in Fig. 7.

In this model, the part of the diagram until the parabola peak is assumed to be a second order parabola where the stress is obtained according to Eq. (10), and the falling branch is linear, which is calculated from Eq. (11).

$$f_c = f'_c \left[2 \frac{\epsilon_c}{\epsilon'_c} - \left(\frac{\epsilon_c}{\epsilon'_c} \right)^2 \right] \quad (10)$$

$$f_c = f'_c \left[1 - 0.15 \left(\frac{\epsilon_c - \epsilon'_c}{\epsilon_{cu} - \epsilon'_c} \right) \right] \quad (11)$$

where ϵ_{cu} is ultimate strain of concrete and ϵ'_c is the strain at f'_c , which is calculated as:

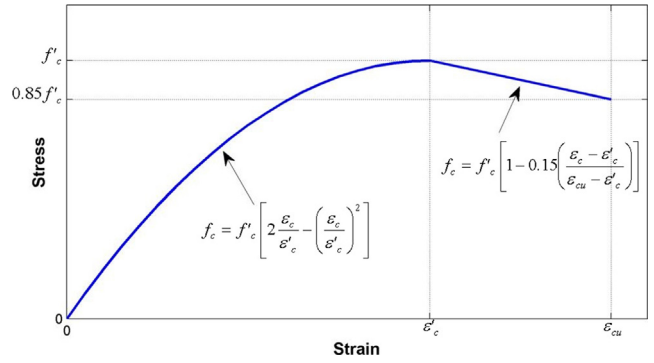


Fig. 7. Stress-strain curve of concrete introduced by Hognestad [46].

$$\epsilon'_c = \frac{1.8f'_c}{E_c} \quad (12)$$

where E_c is the elastic modulus of concrete. For a concrete with a specific weight of w_c , E_c is calculated as (a) or (b) [45]:

(a) For values of w_c between 14.1 and 25.1 KN/m³ (between 90 and 160 lb/ft³)

$$E_c = 44w_c^{1.5} \sqrt{f'_c} \quad (\text{in MPa}) \quad (13)$$

(b) For normal-weight concrete

$$E_c = 4730 \sqrt{f'_c} \quad (\text{in MPa}) \quad (14)$$

(Note: 1 MPa = 145 psi).

If using AMF to hardened concrete causes f'_c to change into $\alpha f'_c$, E_c and ϵ'_c change, respectively, into $\sqrt{\alpha} E_c$ and $\sqrt{\alpha} \epsilon'_c$. So, the relation between stress and strain in the presence of AMF is obtained, modifying the Eq. (10), as follows:

$$f_c = \sqrt{\alpha} f'_c \left[2 \frac{\epsilon_c}{\epsilon'_c} - \frac{1}{\sqrt{\alpha}} \left(\frac{\epsilon_c}{\epsilon'_c} \right)^2 \right] \quad (15)$$

According to Eq. (15), if $\alpha > 1$, the compressive stress needed to reach a specific strain is higher in the presence of AMF than in the absence of it.

According to the results of PoM specimens the amount of α is about 1.078. The Hognestad stress-strain diagrams when AMF = 0 and 0.5 T (related to the NM and PoM specimens, respectively) are shown in Fig. 8(a). Where ϵ'_c for AMF = 0 T is assumed to be 0.002, and f'_c for each case is considered, approximately, equal to its cube strength given in Table 5.

Imagine that a concrete structure with a smart controlling system is designed, so that when strain in a specific concrete element reaches, for example, $0.7\epsilon'_c$ at point (A) shown in Fig. 8(b), it is subjected to AMF. If AMF suddenly increases from 0 to 0.5 T, it is theoretically expected the diagram continues from (A) to (B). But, in fact this is impossible, because of the cracks appeared in concrete as well as its plastic behavior. So, in this condition, the diagram continues from (A) to (B'), which despite increase in stress there is no or a slight increase in strain. This implies that modulus of elasticity and consequently, stiffness of concrete is very large in this part. If AMF gradually increases until it reaches 0.5 T, the diagram would continue from A to a point like (B''). After AMF is fixed at 0.5 T, the diagram continues until concrete collapses at (D).

- RC beam ductility

According to the results of previous studies, it can be said that any effort to enhance concrete strength yields an increase in RC member ductility [47–49]. So using AMF in some critical regions

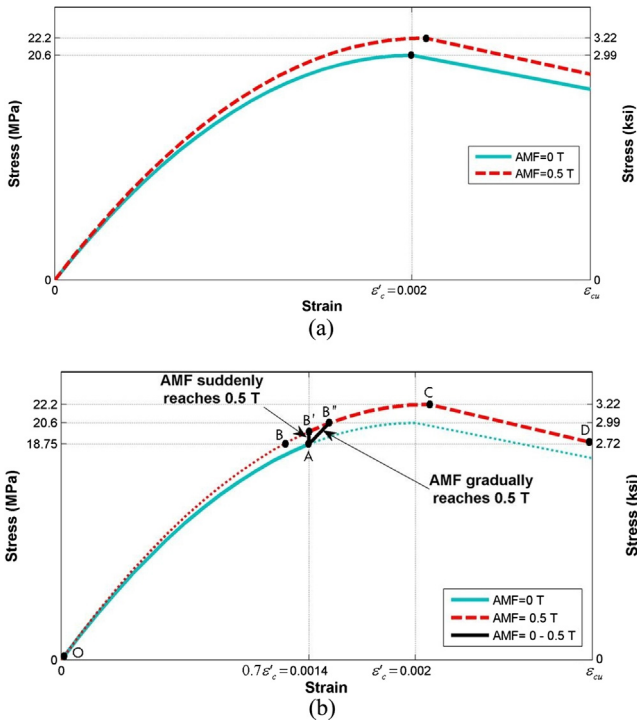


Fig. 8. a) The Hognestad stress-strain diagrams when AMF is 0 and 0.5 T, b) The effect of applying AMF to hardened concrete from $\epsilon_c = 0.7\epsilon_c^d$ onwards, on concrete structure behavior. (Note: 1 MPa = 0.145 ksi).

of smart structures such as beam column joints subjected to cyclic loads will be helpful.

- Nominal moment strength

The nominal moment strength of a rectangular RC beam is calculated using Eq. (16).

$$M_n = \rho f_y b d^2 \left(1 - 0.59 \rho \frac{f_y}{f'_c} \right) \quad (16)$$

where

ρ = tension reinforcement ratio.

b = width of beam.

d = effective depth of beam.

When AMF is applied to concrete, f'_c is changed, approximately, into $1.078f'_c$. So, the nominal moment strength of beam increases and is obtained as follows:

$$M_n = \rho f_y b d^2 \left(1 - 0.547 \rho \frac{f_y}{f'_c} \right) \quad (17)$$

4.3. Feasibility of this method for large-scale RC structures

It seems using this technique in large-scale RC members practically is feasible thanks to presence of steel reinforcement. As stated earlier, magnetic reluctance of iron is very low compared to free space or concrete itself. So, some special reinforcing bars can be chosen to form gapped magnetic circuits and to carry the applied AMF to the locations of interest, while acting as reinforcement. The example schematically shown in Fig. 9 clarifies the idea more easily. Since these bars can have a dual function (AMF carrying and reinforcing), the building cost of this generation of smart structures is not so high. Note that the major issue about these structures is to keep the magnetic leakage as low as possible.

Using this method makes it possible to take control of displacement and failure mode of concrete structures under cyclic loads, i.e. switching AMF on with load applied in one direction, and switching it off when the load is in the opposite one. Hence, the stiffness for the opposite directions are different, changing the hysteresis loop of the element into a non-symmetrical one and making the element to deform in the desired direction.

5. Conclusions

Based on the results of this exploratory investigation under the effect of AMF of frequency 50 Hz and power 0.5 T on compressive properties of concrete, the following conclusions are drawn:

1. Applying AMF to ready mixed concrete has a marginal effect on the compressive.
2. Exposing hardened concrete to AMF increases its compressive strength up to 7.77%.
3. The results concerning with the effect of applying AMF to hardened concrete can lead to developing a new method to take control of behavior of large-scale concrete buildings in real

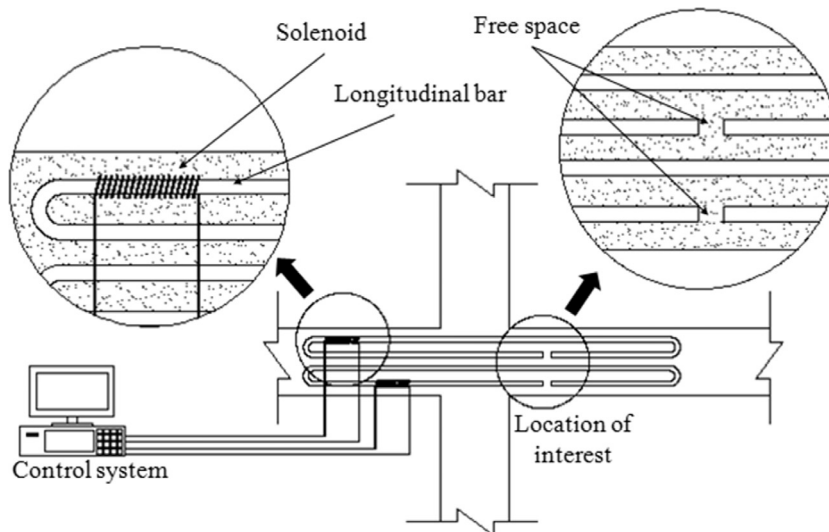


Fig. 9. A smart RC element comprising gapped magnetic circuits.

time, through adjusting stiffness and ductility of some special structural elements, using AMF when strong dynamic forces occur.

- There are some advantages in using this technique for smart concrete structures over some existing methods such as: not being too expensive, no need for actuator embedding in concrete, remove of worries about element load-bearing capacity reduction due to actuator installation.

Acknowledgments

The authors are thankful to the laboratory technician, Mr. M. Bakhshaii, department of Civil Eng. of Semnan University, departments of Civil Eng. and Electrical Eng. of Hakim Sabzevari University, The head of the company of Danesh Pajooan Paya and the Professor and director of the Electric Machines laboratory at Hakim Sanzevari University, Mr. H. Ghalenoei.

References

- L. Senff, D. Hotza, S. Lucas, V.M. Ferreira, J.A. Labrincha, Effect of nano-SiO₂ and nano-TiO₂ addition on the rheological behavior and the hardened properties of cement mortars, *Mater. Sci. Eng. A* 532 (2012) 354–361.
- J.M. Ko, Y.Q. Ni, Technology developments in structural health monitoring of large-scale bridges, *Eng. Struct.* 27 (12) (2005) 1715–1725.
- P.C. Chang, A. Flatau, S.C. Liu, Review paper: health monitoring of civil infrastructure, *Struct. Health Monit.* 2 (3) (2003) 257–267.
- C.K.Y. Leung, K.T. Wan, D. Inaudi, X. Bao, W. Habel, Z. Zhou, J. Ou, M. Ghandehari, H.C. Wu, M. Imai, Review: optical fiber sensors for civil engineering applications, *Mater. Struct.* 48 (4) (2015) 871–906.
- M. Perry, Z. Yan, Z. Sun, L. Zhang, P. Niewczas, M. Johnston, High stress monitoring of prestressing tendons in nuclear concrete vessels using fibre-optic sensors, *Nucl. Eng. Des.* 268 (2014) 35–40.
- G. Uva, F. Porco, A. Fiore, G. Porco, Structural monitoring using fiber optic sensors of a pre-stressed concrete viaduct during construction phases, *Case Stud. Nondestruct. Test. Eval.* 2 (2014) 27–37.
- B. Dong, Y. Liu, L. Qin, Y. Wang, Y. Fang, F. Xing, X. Chen, In situ stress monitoring of the concrete beam under static loading with cement-based piezoelectric sensors, *Nondestruct. Test. Eval.* 30 (4) (2015) 312–326.
- C.G. Karayannis, C.E. Chalioris, G.M. Angeli, N.A. Papadopoulos, M.J. Fawata, C.P. Providakis, Experimental damage evaluation of reinforced concrete steel bars using piezoelectric sensors, *Constr. Build. Mater.* 105 (2016) 227–244.
- D. Xu, S. Banerjee, Y. Wang, S. Huang, X. Cheng, Temperature and loading effects of embedded smart piezoelectric sensor for health monitoring of concrete structures, *Constr. Build. Mater.* 76 (February 2015) 187–193.
- Z.D. Xu, Y.P. Shen, Y.Q. Guo, Semi-active control of structures incorporated with magnetorheological dampers using neural networks, *Smart Mater. Struct.* 12 (1) (2003) 80–87.
- S.H. Lim, B.G. Prusty, G. Pearce, D. Kelly, R.S. Thomson, Study of magnetorheological fluids towards smart energy absorption of composite structures for crashworthiness, *Mech. Adv. Mater. Struct.* 23 (5) (2016) 538–544.
- L. Jingzhou, S. Congya, L. Qingbin, L. Fengli, W. Fengda, Theoretical investigation on natural frequency of electrorheological material based adaptive mortar beam structures using concentrated compliance method, *J. Basic Sci. Eng.* 4 (2009) 558–565.
- M.M. Soleymani, M.A. Hajabasi, S. Elahi Mahani, Free vibrations analysis of a sandwich rectangular plate with electrorheological fluid core, *J. Comput. Appl. Res. Mech. Eng.* 5 (1) (2015) 71–81.
- Q. Chen, B. Andrawe, Monotonic and cyclic experimental testing of concrete confined with shape memory alloy spirals, in: *Proceedings of 10th US National Conference on Earthquake Engineering*, July 21–25, 2014, Anchorage, Alaska, United States.
- J.M. Jani, M. Leary, A. Subic, M.A. Gibson, A review of shape memory alloy research, applications and opportunities, *Mater. Des.* 56 (2014) 1078–1113.
- H. Baier, Approaches and technologies for optimal control-structure-interaction in smart structures, *Trans. Built Environ.* 19 (1996) 323–335.
- B.N. Agrawal, M.A. Elshafei, G. Song, Adaptive antenna shape control using piezoelectric actuators, *Acta Astronaut.* 40 (11) (1997) 821–826.
- S.C. Choi, J.S. Park, J.H. Kim, Active damping of rotating composite thin-walled beams using MFC actuators and PVDF sensors, *Compos. Struct.* 76 (4) (2006) 362–374.
- M.C. Ray, R. Balaji, Active structural-acoustic control of laminated cylindrical panels using smart damping treatment, *Int. J. Mech. Sci.* 49 (9) (2007) 1001–1017.
- Z. Wu, X.P. Qing, F.K. Chang, Damage detection for composite laminate plates with a distributed hybrid PZT/FBG sensor network, *J. Intell. Mater. Syst. Struct.* 20 (9) (2009) 1069–1077.
- D. Mayer, H. Atzrodt, S. Herold, M. Thomaier, An approach for the model based monitoring of piezoelectric actuators, *Comput. Struct.* 86 (3–5) (2008) 314–321.
- Z. Li, P.M. Bainum, Vibration control of flexible spacecraft integrating a momentum exchange controller and a distributed piezoelectric actuator, *J. Sound Vib.* 177 (4) (1994) 539–553.
- E.F. Sheta, R.W. Moses, L.J. Huttshell, Active smart material control system for buffet alleviation, *J. Sound Vib.* 292 (3–5) (2006) 854–868.
- L. Zhou, J. Sun, X.J. Zheng, S.F. Deng, J.H. Zhao, S.T. Peng, Y. Zhang, X.Y. Wang, H. B. Cheng, A model for the energy harvesting performance of shear mode piezoelectric cantilever, *Sens. Actuators A* 179 (2012) 85–192.
- A. Messineo, A. Alaimo, M. Denaro, D. Ticali, Piezoelectric bender transducers for energy harvesting applications, *Energy Procedia* 14 (2012) 39–44.
- Y. Goldfeld, O. Rabinovitch, T. Quadflieg, T. Gries, Integrated Monitoring of TRC Using Carbon Fibers, in: *Proceedings of the 11th International Symposium on Ferrocement and 3rd ICTRC International Conference on Textile Reinforced Concrete*, Aachen, Germany, June 2015, pp. 327–334.
- B.S.K. Reddy, V.G. Ghorpade, H.S. Rao, Effect of magnetic field exposure time on workability and compressive strength of magnetic water concrete, *Int. J. Adv. Eng. Technol.* 4 (3) (2013) 120–122.
- R. Cai, H. Yang, J. He, W. Zhu, The effects of magnetic fields on water molecular hydrogen bonds, *J. Mol. Struct.* 938 (1–3) (2009) 15–19.
- A.R. Soltani Todeshki, H. RaeisiVanani, M. Shayannejad, K. Ostad Ali Askari, Effects of magnetized municipal effluent on some chemical properties of soil in furrow irrigation, *Int. J. Agric. Crop Sci.* 8 (3) (2015) 482–489.
- H. Afshin, M. Gholizadeh, N. Khorshidi, Improving mechanical properties of high strength concrete by magnetic water technology, *J. Sci. Iranica Trans.* A 17 (1) (2010) 74–79.
- M. Gholizadeh, H. Arabshahi, The effect of magnetic water on strength parameters of concrete, *J. Eng. Technol. Res.* 3 (3) (2011) 77–81.
- N. Khorshidi, M. Ansari, M. Bayat, An investigation of water magnetization and its influence on some concrete specificities like fluidity and compressive strength, *Comput. Concr.* 13 (5) (2014) 649–657.
- Y.R. Tawfic, W. Abdelmoez, The influence of “water magnetization” on fresh and hardened concrete properties, *Int. J. Civil Eng. Technol. (IJCIET)* 4 (6) (2013) 31–43.
- S.M. Ahmed, Effect of magnetic water on engineering properties of concrete, *J. Al-Rafidain Eng.* 7 (1) (2009) 71–82.
- N. Su, C.-F. Wu, Effect of magnetic field treated water on mortar and concrete containing fly ash, *Cem. Concr. Compos.* 25 (7) (2003) 681–688.
- N. Su, Y.-H. Wu, C.-Y. Mar, Effect of magnetic water on the engineering properties of concrete containing granulated blast-furnace slag, *Cem. Concr. Res.* 30 (4) (2000) 599–605.
- B.S.K. Reddy, V.G. Ghorpade, H.S. Rao, Influence of magnetic water on strength properties of concrete, *Indian J. Sci. Technol.* 7 (1) (2014) 14–18.
- M. Kciuk, R. Turczyn, Properties and application of magnetorheological fluids, *J. Achiev. Mater. Manuf. Eng.* 18 (1–2) (2006) 127–130.
- S.D. Nair, R.D. Ferron, Set-on-demand concrete, *Cem. Concr. Res.* 57 (2014) 13–27.
- J.J. Soto-Bernal, R. Gonzalez-Mota, I. Rosales, J.A. Ortiz-Lozano, Effects of static magnetic fields on the physical, mechanical, and microstructural properties of cement pastes, *Adv. Mater. Sci. Eng.* 2015 (2015) 1–9.
- W. Arkadiew, Eine Theorie des elektromagnetischen feldes in den ferromagnetischen metallen, *Physik. Z.* 14 (19) (1913) 928–934.
- K. Küpfmüller, Einführung in Die Theoretische Elektrotechnik, Springer-Verlag, Berlin, 1959.
- U.A. Bakshi, M.V. Bakshi, Magnetic circuits, in: *Magnetic Circuits and Transformers*, Technical Publications, India, 2008, pp. 1–48.
- ASTM C109/C109M-13, Standard Test Method for Compressive Strength of Hydraulic Cement Mortars (Using 2-in. or [50-mm] Cube Specimens), ASTM International, West Conshohocken, PA, 2013.
- ACI318-14, Building Code Requirements for Structural Concrete and Commentary (ACI 318R-14), American Concrete Institute, Farmington Hills, MI, USA, 2014.
- E. Hognestad, N.W. Hanson, D. McHenry, Concrete stress distribution in ultimate strength design, *ACI J.* 52 (6) (1955) 455–479.
- N. Ganesan, P.V. Indira, M.V. Sabeena, Behaviour of hybrid fibre reinforced concrete beam-column joints under reverse cyclic loads, *Mater. Des.* 54 (2014) 686–693.
- R. Pendyala, P. Mendis, I. Patnaikuni, Full-range behavior of high-strength concrete flexural members: comparison of ductility parameters of high and normal-strength concrete members, *ACI Struct. J.* 93 (1) (1996) 30–35.
- M.A. Mansur, M.S. Chin, T.H. Wee, Flexural behavior of high-strength concrete beams, *ACI Struct. J.* 94 (6) (1997) 663–674.